

## Decay Kinetics of the 4.4 eV Photoluminescence Associated with the Two States of Oxygen-Deficient-Type Defect in Amorphous SiO<sub>2</sub>

Hiroyuki Nishikawa, Eiki Watanabe, and Daisuke Ito

*Department of Electrical Engineering, Tokyo Metropolitan University, 1-1 Minami-Osawa, Hachioji, Tokyo 192-03, Japan*

Yoshimichi Ohki

*Department of Electrical Engineering, Waseda University, 3-4-1 Ohkubo, Shinjuku-ku, Tokyo 169, Japan*

(Received 24 November 1993)

We present the first observation of 4.4 eV photoluminescence (PL) decay in an oxygen-deficient-type silica excited with ultraviolet and vacuum ultraviolet photons from synchrotron radiation. The lifetime of the 4.4 eV PL is 4.2, 4.3, and 2.1 ns for the 5.0, 6.9, and 7.6 eV excitations, respectively, indicating the presence of multiple decay channels. This can be explained by an energy diagram involving the interconversion between two states of the oxygen-deficient-type defect.

PACS numbers: 78.55.Hx, 42.70.Cc, 61.80.Ba

Point defects in amorphous silicon dioxide (*a*-SiO<sub>2</sub>) have long been attracting much attention [1,2], because of their importance as materials for various technological applications, such as optical waveguides, gate oxides for metal-oxide-semiconductor (MOS) devices, and so on. With the recognition that diamagnetic defects can be potential precursors of photon-induced and radiation-induced paramagnetic defects [3–6], characterization of diamagnetic defects has become of urgent importance.

Compared with the well characterized paramagnetic defects by electron-spin-resonance (ESR) spectroscopy [1], diamagnetic defects in *a*-SiO<sub>2</sub> have been less understood [2]. The oxygen-deficient-type defect can be regarded as one of the most important defects in as-manufactured oxygen-deficient silicas [2], in ion-bombarded and neutron-irradiated silicas [2], and in thermally grown oxides on silicon [7], though the structural origin is highly controversial [2,8]. Because of the lack of a structural sensitive probe such as ESR technique for paramagnetic defects, diamagnetic defects associated with oxygen deficiency in *a*-SiO<sub>2</sub> have been studied mainly on the basis of optical data and theoretical calculations [2,8–16]. Optical absorption bands at 5.0 and 7.6 eV, and photoluminescence (PL) bands at 2.7 and 4.4 eV have been associated with the oxygen deficiency in high-purity silica [8,11–14]. Photoluminescence excitation (PLE) measurements of the 4.4 eV PL in a neutron-irradiated silica using a hydrogen discharge lamp have shown a peak around 7.6 eV [9]. Time-resolved PL measurements with pulsed excitation using excimer lasers have revealed that the 2.7 eV band is a phosphorescence with lifetime of  $\tau \approx 10$  ms, while the 4.4 eV band is a fluorescence with lifetime of  $\tau$  shorter than 10 ns [10]. To date, two structural models have been proposed for these absorption and PL bands; oxygen vacancy [2,11–14] and twofold coordinated silicon [8,17], which are commonly denoted as  $\equiv\text{Si-Si}\equiv$  and  $\text{O}\cdot\ddot{\text{S}}\text{i}\cdot\text{O}$ , respectively (the symbols “ $\equiv$ ” and “ $\cdot\cdot$ ” denote bonds to three separate oxygens and lone-pair electrons, respectively). Furthermore, even for

the oxygen vacancy models, there has been an intense debate over the assignment of optical transitions at 5.0 and 7.6 eV [2]. Although such a dispute is partly due to the lack of structural specificity of available optical data, the major problem lies in the difficulty in performing detailed vacuum-ultraviolet (vuv) spectroscopic study near the intrinsic absorption edge of *a*-SiO<sub>2</sub> around 8–9 eV.

Synchrotron radiation (SR) is a powerful tool for the vuv spectroscopic study of wide-band-gap materials such as alkali halides [18], and crystalline [19] and amorphous [6,13,15,20] forms of SiO<sub>2</sub>, since it provides intense and broad spectral emission over the vuv region. Although there have been many reports for the vuv optical absorption in *a*-SiO<sub>2</sub>, there has been little detailed observation of the PL properties in the vuv region, e.g., time-resolved PL measurements with resolution less than 10<sup>-9</sup> s.

We present here the results of uv-vuv spectroscopic studies of the oxygen-deficient-type defects in *a*-SiO<sub>2</sub>. *This report includes the first observation of the decay kinetics of the 4.4 eV PL under uv and vuv excitations.* Our results provide new insight into issues concerning the *nature* of the oxygen-deficient-type defect in *a*-SiO<sub>2</sub>. The data discussed below strongly suggest the presence of the two states of the oxygen-deficient-type defect. We suggest that the conversion of the defect from one configuration to the other upon the excitation at the 7.6 eV band.

In the present study, an oxygen-deficient-type [3–6] high-purity silica glass ([OH] < 1 part per 10<sup>6</sup> [Cl]: 0.3 part per 10<sup>6</sup>) prepared by the soot remelting method [21] was investigated. Optically polished samples with a thickness of 0.7 and 2.5 mm were used. Synchrotron radiation was utilized at BL7B line of UVSOR operated at an electron energy of 750 MeV (Institute for Molecular Science, Okazaki, Japan) equipped with a 1 m Seya-Namioka type monochromator. Vacuum-ultraviolet absorption, PL, and PLE spectra were measured using SR under multibunch operation. Transient behavior of the PL was measured by a time-correlated single photon counting technique using SR under single-bunch opera-

tion (the time interval of SR pulses  $\approx 177.6$  ns). An apparent pulse duration of the SR is  $\approx 550$  ps including time response of the detection system. Emission was dispersed by either a grating monochromator (Jobin-Yvon HR320) or band pass filters (Toshiba KL) and was detected by a photomultiplier (Hamamatsu R955 or R2287U-06). Measurements were carried out at 40–300 K. Before measurements, samples were not exposed to any radiations.

The luminescence intensity  $I_{lum}$  with radiative decay efficiency  $\eta$ , can be given by

$$I_{lum} = \eta I_{abs} = \eta I_{exc} [1 - \exp(-\alpha L)],$$

where the  $I_{abs}$  is the light intensity absorbed at the sample with an absorption coefficient  $\alpha$  and a thickness  $L$ , and the  $I_{exc}$  is the excitation light intensity. Since the  $I_{exc}$  is measured with the photomultiplier coated with sodium salicylate whose fluorescent quantum yield is constant between 4 and 20 eV [22], the  $I_{exc}$  represents the relative numbers of the incident photons. Since the values of the  $I_{exc}$  and  $I_{lum}$  were not calibrated, only the relative values of the  $\eta$  can be obtained.

Figure 1(a) shows the uv-vuv absorption and PL spectra for the oxygen-deficient-type silica observed at 60 K. An absorption band at 5.0 eV is a so-called  $B_2\alpha$  band [11] which is a Gaussian-shaped peak [peak energy ( $E_p$ ) of 5.03 eV and a full width at half maximum (FWHM) of 0.35 eV]. The 7.6 eV band is also Gaussian in shape ( $E_p$ : 7.64 eV, FWHM: 0.52 eV), which is in good ac-

cord with previous reports [11,13]. Figure 1(b) shows the PLE spectrum ( $I_{lum}/I_{exc}$ ) of the 4.4 eV band measured at 60 K. Two PLE components can be seen; one is a symmetrical component about 5.0 eV and the other is an asymmetrical one extending from 6 to 8 eV. The asymmetrical component can be resolved into two components as shown in Fig. 1(b) (broken curves). One is Gaussian in shape centered at 6.88 eV with an FWHM of 0.55 eV, and the other is still asymmetrical extending from 7 to 8 eV. In the case of low absorption region, i.e., the case of  $\alpha L \ll 1$ , the PL intensity can be approximately given by  $I_{lum} \approx \eta I_{exc} \alpha L$ . Thus, the experimentally obtained  $I_{lum}/I_{exc}$  spectrum should be proportional to the absorption coefficient  $\alpha$ . The PLE peak at 5.0 eV, in fact, coincides well with the  $B_2\alpha$  band. The 6.9 eV PLE band should also reflect the shape of the absorption band, though it is presumably masked by the low energy tail of the intense 7.6 eV band. The position of the PLE band at 7–8 eV in Fig. 1(b) also coincides with that of the 7.6 eV band in Fig. 1(a). Since the 7.6 eV band is so intense ( $\alpha L \gg 1$ ) that the value of  $I_{lum}/I_{exc}$  is no longer proportional to the absorption coefficient  $\alpha$ , the PLE band at 7–8 eV is expected to be distorted in shape. Therefore, we attribute the PLE component at 7–8 eV to the 7.6 eV absorption band. This interpretation is consistent with a previous report [9]. Using the relation  $\eta = (I_{lum}/I_{exc}) \times [1 - \exp(-\alpha L)]^{-1}$ , the value of  $\eta$  at 7.6 eV is estimated to be about 1 order of magnitude lower than those of  $\eta$  at 5.0 and 6.9 eV.

Figure 2 shows the decay of the 4.4 eV PL excited at the 5.0, 6.9, and 7.6 eV PLE bands. The 5.0 and 6.9 eV excitations exhibit almost parallel decay curves, while the 7.6 eV excitation shows a faster decay curve. Fitting can be approximately made using a simple exponential function of  $I = I_0 \exp(-t/\tau)$ . We obtained  $\tau \approx 4.2$  ns for the 5.0 eV excitation,  $\tau \approx 4.3$  ns for the 6.9 eV excitation, and  $\tau \approx 2.1$  ns for the 7.6 eV excitation.

We should consider what types of transitions are responsible for these absorption and PL bands. First of all, a question arises as to whether the 5.0 and 7.6 eV absorption bands should be ascribed to one type of defect or two different types of defects [2]. The present study gives the following observations. (I) The 4.4 eV PL band exhibits three PLE bands at 5.0, 6.9, and 7.6 eV, (II) the radiative decay efficiency upon the 7.6 eV excitation is about 1 order of magnitude smaller than those observed upon the 5.0 and 6.9 eV excitations, and (III) the 4.4 eV PL decays faster in the case of 7.6 eV excitation than in the cases of 5.0 and 6.9 eV excitations. Observation (I) suggests that the 7.6 eV excitation can create the same excited states responsible for the 4.4 eV PL as in the cases of 5.0 and 6.9 eV excitations. Observations (II) and (III) show that an additional nonradiative decay channel exists for the case of the 7.6 eV excitation. Based on these observations, we propose an energy diagram which involves two different configurations of the defect shown in Fig. 3.

First, we discuss the energy diagram of the  $C_1$  config-

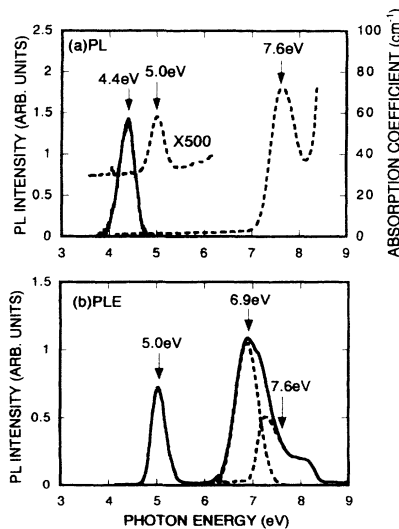


FIG. 1. (a) Photoluminescence (PL) spectrum (solid curve) and ultraviolet and vacuum ultraviolet absorption spectrum (broken curves), and (b) PL excitation (PLE) spectrum (solid curve) observed in an oxygen-deficient-type silica at 60 K. As shown by the broken curves, the peak around 6–8 eV is resolved into two components. Here, the PLE spectra are given by  $I_{lum}/I_{exc}$ , where the  $I_{lum}$  and  $I_{exc}$  are the luminescence and excitation light intensities, respectively.

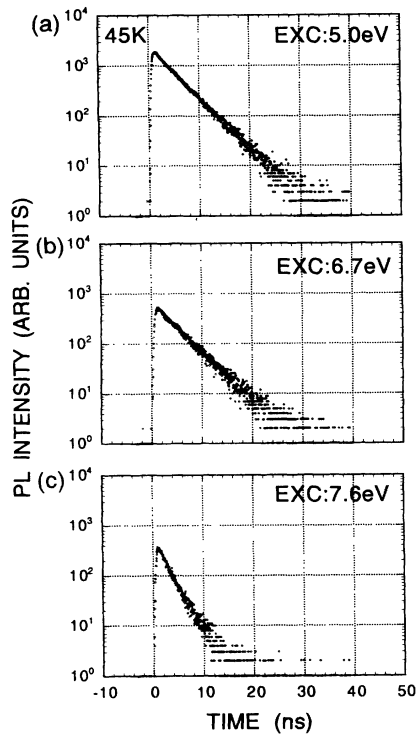


FIG. 2. Decay of the 4.4 eV photoluminescence observed by the excitations of the three PLE bands at (a) 5.0 eV, (b) 6.9 eV, and (c) 7.6 eV. Measurements were carried out at 45 K. Note that for the excitation at the 6.9 eV PLE band, the decay was measured when excited by 6.7 eV photons, in order to avoid the simultaneous excitation at the 7.6 eV band.

uration in Fig. 3(a). The  $S_1$  and  $S_2$  states are associated with the transitions at 5.0 and 6.9 eV, respectively. The emission of 4.4 eV is ascribed to the transition from the  $S_1$  to  $S_0$  states. The lifetime of the 4.4 eV PL is given by  $\tau = (k_2 + k_4)^{-1}$ . The lifetime observed at 290 K (data not shown) is smaller only by about 0.3 ns than the one observed at 45 K. Therefore, the nonradiative decay rate  $k_4$ , which is expected to be temperature dependent, is negligible when compared with the value of  $k_2$ . We can then obtain  $k_2 \approx \tau^{-1} = 2.4 \times 10^8 \text{ s}^{-1}$ , which is consistent with the foregoing assignment of the 4.4 eV PL to singlet-singlet transition ( $S_1 \rightarrow S_0$ ). Slightly longer lifetime of  $\tau \approx 4.3 \text{ ns}$  observed upon the 6.9 eV excitation can be ascribed to the fact that the  $S_1$  population is limited by the nonradiative decay from the  $S_2$  state with a rate constant of  $k_3(S_2 \rightarrow S_1)$ .

It has been reported that the 5.0 eV band is due to the singlet-triplet transitions, which is forbidden by the spin selection rule [11]. An experimental basis for this assignment is the observation of the 4.4 eV PL decay with a relatively long lifetime of  $\tau \approx 100 \mu\text{s}$  upon 5.0 eV excitation. However, as the present result has shown and as already pointed out [8], the data were not reproduced.

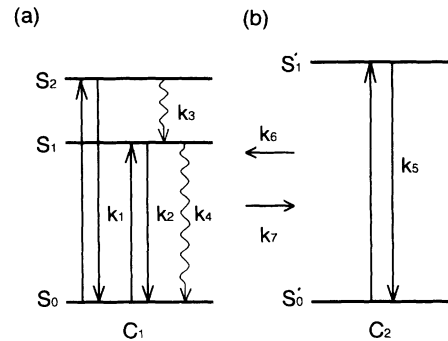


FIG. 3. Schematic energy diagram for observed optical transitions. Two configurations are illustrated: (a)  $C_1$  is luminescent at 4.4 eV ( $S_1 \rightarrow S_0$ ) for the 5.0 eV ( $S_0 \rightarrow S_1$ ) and 6.9 eV ( $S_0 \rightarrow S_2$ ) excitations, and (b)  $C_2$  for the 7.6 eV excitation ( $S'_0 \rightarrow S'_1$ ). Also illustrated is the conversion of oxygen-deficient-type defects from  $C_2$  to  $C_1$  upon the 7.6 eV excitations, followed by reversion back to the  $C_2$  configuration.

Therefore, the value should be revised to  $\tau \approx 4.2 \text{ ns}$ .

Shown in Fig. 3(b) is the energy diagram of the defect in the  $C_2$  configuration where the 7.6 eV band is ascribed to the transition from  $S'_0$  to  $S'_1$  states. Upon the excitation at the 7.6 eV band, we assume the conversion of the defect from the  $C_2$  to  $C_1$  configurations with a rate constant of  $k_6$ , followed by a backreaction with a rate constant of  $k_7$ . Thus the lifetime of the 4.4 eV PL is given by  $\tau = (k_2 + k_4 + k_7)^{-1}$ , which should be shorter than the lifetime of  $\tau = (k_2 + k_4)^{-1}$  for the 5.0 and 6.9 eV excitations. Using the values of  $k_2 + k_4 = 2.4 \times 10^8 \text{ s}^{-1}$  and  $\tau \approx 2.1 \text{ ns}$ , we obtain the value of  $k_7 = 2.4 \times 10^8 \text{ s}^{-1}$  at 45 K. We have previously observed in oxygen-deficient-type silicas the growth of the 5.0 eV band [23] and the partial bleaching of the 7.6 eV band [24] after irradiation with a 7.9 eV excimer laser. This is in good accord with the proposed scheme in Fig. 3. As discussed above, the observed PL decay kinetics, together with the PLE spectra, strongly suggests the presence of the two states of oxygen-deficient-type defect. Although there has been a report of the circumstantial evidence [13], this, to our knowledge, is the first *direct* evidence for the two-state system of the oxygen-deficient-type defect.

Finally, we turn to the structural models for the  $C_1$  and  $C_2$  defects. First, we discuss oxygen vacancy models. The proposed scheme in Fig. 3 is fairly well in agreement with the results of tight-binding calculations reported by O'Reilly and Robertson [25] showing that two types of oxygen vacancies with different Si-Si distances give the optical transitions at 5.85 eV for unrelaxed oxygen vacancy and at 7.6 eV for the relaxed one. The scheme proposed in Fig. 3 is consistent with the previous report on the laser-induced  $E'$  centers [13]. Two types of oxygen vacancies, relaxed and unrelaxed, were assumed to explain the formation of the  $E'$  centers in oxygen-deficient-

type silicas under 5.0 or 6.4 eV excimer laser irradiation [13].

In view of the results of tight-binding calculations [25] and the laser-induced defects [13] cited above, a plausible assignment is  $C_1$  to the unrelaxed oxygen vacancy ( $\equiv\text{Si}\cdots\text{Si}\equiv$ ) and  $C_2$  to the relaxed one ( $\equiv\text{Si-Si}\equiv$ ). Upon excitation at the 7.6 eV band, the two silicon atoms in the relaxed  $C_2$  configuration presumably move apart by the excitation to an antibonding state. The resultant excited  $C_1$  configuration decays either radiatively or non-radiatively, competing with an additional nonradiative decay process, i.e., the reconversion back to the initial relaxed  $C_2$  configuration.

However, any of the considerations given above cannot rule out another structural model, the twofold-coordinated silicon center (O- $\dot{\text{S}}\text{i}$ -O) [8]. Experimental data and the proposed energy diagram [8,26] are basically consistent with the present experimental observation. Based on the nonexponential decay of the 2.7 eV phosphorescence upon 7.6 eV excitation, a complex defect containing twofold coordinated silicon was proposed for the 7.6 eV band [26]. In view of the energy diagram in Fig. 3, the twofold coordinated silicon and the complex defect can be regarded as the  $C_1$  and  $C_2$  defects, respectively. However, the structure of the complex defect, which was attributed to impurity hydrogen and/or chlorine [26], is not evident.

In conclusion, the excitation spectrum and decay kinetics of the 4.4 eV PL band in an oxygen-deficient-type silica were reported for the first time in the uv and vuv regions using SR. The data of the PLE spectrum and the PL decay kinetics strongly suggest that two states of the oxygen-deficient-type defect are involved in the 4.4 eV emission. An energy diagram involving two configurations of the defect is consistent with previous theoretical calculations and experimental data on the laser-induced  $E'$  centers. We suggest the conversion of the oxygen-deficient-type defect from one configuration to the other upon excitation at the 7.6 eV band.

The authors appreciate Professor K. Nagasawa of Shonan Institute of Technology and Dr. F. Tochikubo of Tokyo Metropolitan University for the useful discussion. This work was partly supported by the Joint Studies Program (1992-1994) of the Institute for Molecular Science, UVSOR Facility, and by a Grant-in-Aid from the Ministry of Education, Science and Culture of Japan (No. 05750295).

- [1] D. L. Griscom, in *Defects in Glasses*, edited by F. L. Galeener, D. L. Griscom, and M. J. Weber (Materials Research Society, Pittsburgh, PA, 1986), p. 213.
- [2] D. L. Griscom, in *Proceedings of the Thirty-Third Frequency Control Symposium* (Electronic Industries Association, Washington, DC, 1979), p. 98; J. Ceram. Soc. Jpn. **99**, 923 (1991).
- [3] K. Nagasawa, Y. Hoshi, and Y. Ohki, Jpn. J. Appl. Phys. **26**, 554 (1987).
- [4] H. Nishikawa *et al.*, J. Appl. Phys. **65**, 4672 (1989).
- [5] H. Nishikawa *et al.*, Phys. Rev. B **41**, 7828 (1990).
- [6] H. Nishikawa, R. Nakamura, Y. Ohki, and Y. Hama, Phys. Rev. B **48**, 2968 (1993).
- [7] W. L. Warren, P. M. Lenahan, and C. J. Brinker, J. Non-Cryst. Solids **136**, 151 (1991).
- [8] L. N. Skuja, J. Non-Cryst. Solids **149**, 77 (1992).
- [9] C. M. Gee and M. A. Kastner, Phys. Rev. Lett. **42**, 1765 (1979); **35** & **36**, 927 (1980).
- [10] J. H. Stathis and M. A. Kastner, Phys. Rev. B **35**, 2972 (1987).
- [11] R. Tohmon *et al.*, Phys. Rev. B **39**, 1337 (1989).
- [12] R. Tohmon *et al.*, Phys. Rev. Lett. **62**, 1388 (1989).
- [13] H. Imai *et al.*, Phys. Rev. B **38**, 12772 (1988).
- [14] H. Hosono *et al.*, Phys. Rev. B **44**, 12043 (1991).
- [15] K. Awazu, H. Kawazoe, and K. Muta, J. Appl. Phys. **69**, 4183 (1991); **70**, 69 (1991).
- [16] H. Nishikawa *et al.*, Phys. Rev. B **45**, 586 (1992).
- [17] L. N. Skuja, A. R. Silin, and J. Mares, Phys. Status Solidi (a) **50**, K149 (1978).
- [18] K. Kan'no *et al.*, Phys. Scr. **41**, 120 (1990).
- [19] C. Itoh, K. Tanimura, N. Itoh, and M. Itoh, Phys. Rev. B **39**, 11183 (1989).
- [20] I. P. Kaminow, B. G. Bagley, and C. G. Olson, Appl. Phys. Lett. **32**, 98 (1988).
- [21] See for example, T. Izawa and S. Sudo, *Optical Fibers* (KTK Scientific Publishers, Tokyo, 1987).
- [22] R. Allison, J. Burns, and A. J. Tuzzolino, J. Opt. Soc. Am. **54**, 747 (1964).
- [23] H. Nishikawa *et al.*, in *Proceedings of the Third International Symposium, International Symposium on Structural Imperfections in SiO<sub>2</sub>-based Amorphous Materials*, edited by H. Kawazoe, H. Imagawa, and K. Arai, Transactions of the Materials Research Society of Japan (MRS, Japan, 1992), Vol. 8, p. 120.
- [24] H. Nishikawa, R. Nakamura, Y. Ohki, and Y. Hama, Phys. Rev. B **48**, 15584 (1993).
- [25] E. P. O'Reilly and J. Robertson, Phys. Rev. B **27**, 3780 (1983).
- [26] A. N. Trukhin, L. N. Skuja, A. G. Boganov, and V. S. Rudenko, J. Non-Cryst. Solids **149**, 96 (1992).